RSC Advances

ROYAL SOCIETY OF CHEMISTRY

www.rsc.org/advances

Systhesis of carbon quantum dot-surface modified P25 nanocomposites for photocatalytic degradation of *p*-nitrophenol and acid violet 43

Fengying Zheng,a Zhenhua Wang,a Jie Chen,a ShunXing Li*a,b

[a] *Department of Chemistry and Environmental Science, Minnan Normal University, Zhangzhou 363000, China*

[b] *Fujian Province Key Laboratory of Modern Analytical Science and Separation Technology, Minnan Normal University, Zhangzhou, China, 363000*

*E-mail: lishunxing@mnnu.edu.cn; shunxing_li@aliyun.com

Tel.: +86 596 2591395

Fax: +86 596 2591395

ABSTRACT

A new efficient and stable visible light driven photocatalyst, carbon quantum dots (CQDs) -surface modified P25 nanocomposite, was successfully prepared by chemical adsorption of CQDs onto the surface of TiO_2 nanoparticles and then used for water treatment. The photocatalyst was characterized by X-ray powder diffraction, transmission electron microscope, X-ray photoelectron spectroscopy, infrared spectrometer, thermo gravimetric analyzer, and UV-Vis spectra. After the modification of titanium dioxide with carbon quantum dots, the UV-Vis wavelength response range expanded from 390 nm to 420 nm by accelerating the photogenerated electron transfer from carbon quantum dots to titanium dioxide, and the band gap decreased from 3.08 ev to 2.87 ev. In addition, a blue shift of bind energy was observed, namely, 0.6 eV for Ti $_2p_{1/2}$ and 0.7 eV for Ti $_{2p3/2}$, respectively. Furthermore, compared with pure titanium dioxide, after irradiating for 2.5 h, the photodegradation ratio of acid violet 43 and *p*-nitrophenol have been enhanced from 60% to 93% and from 89% to 96%, respectively. Moreover, after five times circles, the stability of the photocatalyst has been maintained due to the strong interaction between carbon quantum dots and titanium dioxide.

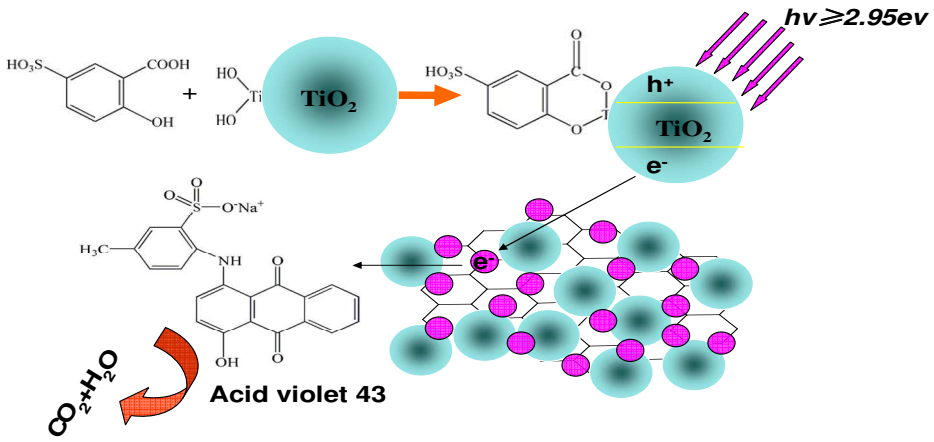

Synthesis of carbon quantum dot-surface modified P25 nanocomposites for photocatalytic degradation of *p*-nitrophenol and acid violet 43

Fengying Zheng,[a] Zhenhua Wang,[a] Jie Chen,[a] ShunXing Li*[a,b]

[a] Department of Chemistry and Environmental Science, Minnan Normal University, Zhangzhou China, 363000

[b] Fujian Province Key Laboratory of Modern Analytical Science and Separation Technology, Minnan Normal University, Zhangzhou, China, 363000

Correspondence to: S. X. Li

*E-mail: lishunxing@munu.edu.cn; shunxing_li@aliyun.com

Tel.: +86 596 2591395

Fax: +86 596 2591395

ABSTRACT

A new efficient and stable visible light driven photocatalyst, carbon quantum dots (CQDs) -surface modified P25 nanocomposite, was successfully prepared by chemical adsorption of CQDs onto the surface of TiO_2 nanoparticles and then used for water treatment. The photocatalyst was characterized by X-ray powder diffraction, transmission electron microscope, X-ray photoelectron spectroscopy, infrared spectrometer, thermo gravimetric analyzer, and UV-Vis spectra. After the modification of titanium dioxide with carbon quantum dots, the UV-Vis wavelength response range expanded from 390 nm to 420 nm by accelerating the photogenerated electron transfer from carbon quantum dots to titanium dioxide, and the band gap decreased from 3.08 ev to 2.87 ev. In addition, a blue shift of bind energy was observed, namely, 0.6 eV for Ti $_2p_{1/2}$ and 0.7 eV for Ti $_{2p3/2}$, respectively. Furthermore, compared with pure titanium dioxide, after irradiating for 2.5 h, the photodegradation ratio of acid violet 43 and *p*-nitrophenol have been enhanced from 60% to 93% and from 89% to 96%, respectively. Moreover, after five times circles, the stability of the photocatalyst has been maintained due to the strong interaction between carbon quantum dots and titanium dioxide.

Keyword: Quantum dots; Titanium; Surface modification; Photodegradation; Aromatic pollutants

1 Introduction

The total degradation of organic pollutants (pesticides, herbicides, insecticides, fungicides, dyes, etc....) is the main field of water photocatalytic decontamination.[1] The commercial pyrogenic titania P25 (Evonik) is routinely used as a benchmark photocatalyst due to its unselective fairly good photoactivity towards wide spectra of pollutants, commercial availability, and low cost.[2] Because of the broad energy gap of TiO_2 (Eg = 3.20~4.50 eV), the photocatalytic process should be induced by the ultraviolet light ($\lambda \leq 387$ nm).[3] Surface modification of TiO_2 has been used to narrow its band gap and extend its UV-vis wavelength response range.[3-5] Semiconductor quantum dots (QDs), including CdS, CdSe, PbS, PbSe, InP, InAs, and CdTe, have been assembled onto porous films, nanotubes, nanowires, and nanoparticles of TiO_2 and then used as photocatalyst (QDs/TiO_2) for water splitting or the development of solar cell devices.[6-8] The unique features of QDs/TiO_2 include high optical absorption coefficient, narrow band gap, and extended photostability, which underlie efficient harvesting of light energy.[6] In addition, QDs can form a type-II staggered band interface with TiO_2 for efficient charge separation and transfer.[9] Because of serious photocorrosion,[9] harmful heavy metal ions can be released from QDs/TiO_2 into the solutions[10] and then the photodegradation efficiency of these heavy metal-based QDs was decreased. Furthermore, the

application of QDs/TiO_2 on water treatment is limited by its cytotoxicity.[10]

The carbon quantum dots (CQDs) are new functional carbon-aceous materials. Compared to conventional dye molecules and QDs, CQDs are superior in low toxicity, low cost, environmentally friendly, biocompatibility, and extensive source.[11] Herein, a new efficient and stable visible light driven photocatalyst (CQDs-surface modified P25 nanocomposites) is prepared by chemical adsorption of CQDs onto the surface of TiO_2 nanoparticles and then used for water treatment. The surface modification of TiO_2 with CQDs can effectively extend the photoresponse of TiO_2 to the visible-light region, accelerate the electron transfer between CQDs and TiO_2, and improve the affinity between photocatalyst and aromatic pollutants, including typical dye (acid violet 43, AV 43) and *p*-nitrophenol (PNP). Enhanced visible-light photocatalytic performance is therefore expected.

2. Experiments

2.1 Materials

The P25-TiO_2 was purchased from Degussa, with the average particle size of 21 nm. AV 43 (CAS No. 4430-18-6) was purchased from the chemical reagent station in Tokyo, Japan. PNP was obtained from Aldrich Chemical Co. (USA). All other chemicals were of the highest purity commercially available. De-ionized water was purified with a

Milli-Q water ion-exchange system (Millipore Co., USA) for a resistivity of 18 MΩ·cm and used throughout the experime.

2.2 Preparation of CQDs and CQDs/TiO_2 composites

An electrolytic denudation method was used for the synthesis of CQDs and its procedures were reported by Li et al..[12] In a beaker, the electrolyte of the electrochemical process was prepared by mixing ehanol/H_2O (100 mL; volume ratio=99.5:0.5) with 0.4 g of NaOH. By using graphite rods (diameter about 0.5 cm) as both anode and cathode, CQDs was synthesized with a current intensity 80 mA for 4 hours. The raw CQDs solution was treated by adding 7.0 g of $MgSO_4$, stirred for 20 min, and then stored for 24 h to remove the water and salt. The residue of $MgSO_4$ was detached by the filtration. Afterwards, the purified CQDs solution was rotary evaporated to remove the ethanol, carbon quantum dots were redispersed in water.

After dispersing of P25 powder into 45 mL of water, 5 mL of purified CQDs solution was added with stirring for 4 h, vacuum filtered, dried at 60 °C overnight, and then CQDs/TiO_2 was obtained. The loading of CQDs was calculated by thermogravimetric analysis (TGA).

2.3 Photocatalytic test

The photocatalytic activity of the photocatalysts (P25 and CQDs/P25) were evaluated by the photodegradation of AV and PNP. A 60 W high-pressure mercury lamp placed 10 cm away from the reaction vessel

was used as the light source. The illumination intensity was 53 mW/cm^2. A 100 mL beaker was used as a photoreactor, into which 100mL 0.15 mmol/L of AV 43 (or 30 mg/L of PNP) with a certain pH value and the designed concentration of CQDs/P25 (or P25) were added. The photoreactor was equipped with an electromagnetic stirrer. After being irradiated for a period of time, 3 mL of the reaction solution were taken out and centrifuged at 10000 rpm to remove the photocatalyst. The concentration of AV 43 in the filtrates were determined spectrophotometrically at λ=560 nm. After adjusting the pH value of the filtrates as 9.0, the concentrations of PNP were determined by measuring the absorbance at 400 nm.

2.4 Characterization

The crystalline phase and crystal size of the photocatalysts (P25 and CQDs/P25) were determined by X-ray diffraction (XRD, Cu Ka, 40kV, 100 mA, D/max2400 Rigaku, Japan MAC Science). The morphologies of the photocatalysts were observed with transmission electron microscope (TEM, Hitachi-600-2). Using an Aglient 8453 UV/Vis diode array spectrophometer, the diffuse reflectance UV-visible spectra were obtained for dry pressed disk samples, which were prepared by mixing the photocatalysts and $BaSO_4$ and its scans range was 300-700 nm. After being Infrared absorptions were studied by a Nicolet 360 IR spectrometer for judging the functional groups of P25 and CQDs/P25. Samples were

125 mixed with potassium bromide, and the content of the samples were kept
126 around 1.0%.

127 **2.5 Data Processing**

128 The photocatalytic degradation ratio was calculated by $(A_0 -$
129 $A_t)/A_0 \times 100$. The value of A was proportional to the concentration of AV
130 43 and PNP based on Beer–Lambert law. A_0 was the initial absorbancy of
131 the specimen, and A*t* was the absorbancy of the specimen when the
132 photocatalytic degradation time is *t*.

133 **3. Results and discuss**

134 **3.1 TEM characterization**

135 As shown in Fig. 1a, the size distribution of CQDs was narrow in the
136 range of 2-10 nm. The dispersibility of CQDs in water was good, i.e.,
137 without larger aggregates, indicating that CQDs were protected by some
138 function groups. From the HRTEM image (seen in Fig.1b), the crystal
139 lattice of graphite was clearly observed and similar results were reported
140 by Zhou et al..[13] After mixing of CQDs and P25, CQDs were found onto
141 the surface of P25 in some area (seen in Fig. 1c and d).

142

143 **Fig. 1**

144

145 **3.2 TGA data**

146 The thermogravimetric analysis (TGA) was conducted to confirm

whether CQDs was combined with P25 in the CQDs/P25 sample and the results for P25 and CQDs/P25 were shown in Fig. 2. TGA of P25 showed a 3.3 wt% total weight loss in two apparent steps on heating to 600 °C. The mass loss between 205 °C and 265 °C was due to the release of surface hydroxylated species. The TGA curve of CQDs/P25 could be divided into three apparent steps with a 8.1 wt% total weight loss. The first step was similar as P25, mass loss (3.3 wt%) and its reason was same, but its temperature range was decreased from 60 °C (i.e., 205-265 °C) to 35 °C (i.e., 185-220 °C). The 4.8 wt% weight loss between 210 °C and 510 °C was due to the slow combustion of carbon in the CQDs, so the CQDs loading was about 4.8%.

Fig. 2

3.3 XRD analysis

The XRD patterns of P25 and CQDs/TiO_2 were shown in Fig. 3. The phase structure in P25 samples were the coexistence of anatase and rutile. However, no carbon diffraction peaks could be observed in the CQDs/TiO_2 sample, because the size of CQDs was small (2-10 nm) and the loading of CQDs was only about 4.8%.

Fig. 3

3.4 FT-IR analysis

To discuss the combination mode between CQDs and P25, the functional groups in P25 and CQDs/P25 were characterized and compared in Fig. 4. The hydroxyl groups and carboxyl groups were reported on the surface of CQDs under alkaline environment.[12] The peak around 3380 cm^{-1} was overlapped by the hydroxyls on the surface of P25 and CQDs. After surface modification with CQDs, the obvious change on the functional groups of P25 was the appearance of a peak around 1380 cm^{-1}. This peak was conjectured to be –COOTi- group, which originated from the esterification between the carboxyl groups from CQDs and the hydroxyls from P25. In addition, the strong hydrogen bonds could form between the hydroxyl groups from thre surface of CQDs and TiO_2. So, the combination between CQDs and TiO_2 was chemical adsorption and it promoted the electronic conduction and connective stability.

Fig. 4

3.5 UV-Vis diffuse reflection absorption

Fig. 5 gave the UV–Vis diffuse reflection absorption spectra of P25, CQDs and CQDs/P25. Compared with the pure P25, its UV-vis wavelength response range was expanded from 390 nm to 420 nm, which

might be contributed by the visible light absorption of CQDs. The E_g (band gap energy) value of P25 could be narrowed by the surface modification with CQDs and its band gap was changed from 3.08 ev to 2.87 ev. This absorption feature suggested that this CQDs/TiO_2 catalyst could be activated by visible light and the utilization of sunlight were improved.

Fig. 5

3.6 XPS analysis

The XPS spectral of Ti_{2p} region were shown in Fig. 6. The bind energy of Ti $_2p_{1/2}$ and Ti $_{2p3/2}$ positioned around 464 eV and 458 eV. Compared to the binding energy of 464.6 eV and 458.7 eV in P25 sample, there was a blue-shift of 0.6 eV and 0.7 eV for the CQDs/P25 sample. Hence, the photogenerated electron could be injected easily and rapidly into the CQDs and following departed away to the oxygen in water through the strong interaction between CQDs and TiO_2. The CQDs offered a high-speed channel for the photogenerated electron and reduced the probability of electron-hole recombination.

Fig. 6

3.7 Photodegradation test

Using CQDs/P25 as the photocatalyst, the effect of pH value and catalyst concentration on the degradation ratio of AV 43 and PNP was shown in Fig. 7 and 8. The influence trends of pH value on the photodegradation of AV 43 and PNP were similar and the optimum pH value was same as 3.0. With the increasing of the concentration of CQDs/P25 from 0.10 to 3.00 g/L, the active sites for the production of ·OH radicals were increased, the photodegradation ratio of AV 43 and PNP was increased, the increasing level were more significant in the range of 0.1-1.0 g/L for AV 43 and 0.1-2.0 g/L for PNP. So the adopted concentration of CQDs/P25 was 1.0 g/L for AV 43 and 2.0 g/L for PNP in the photocatalytic experiments.

Fig. 7

Fig. 8

To evaluate and compare the photocatalytic performance of P25 and CQDs/P25 in aqueous contaminants, the decomposition of AV 43 and PNP was used as probe photoreactions and the results were shown in Fig. 9. The photodegradation ratio of AV 43 and PNP could be increased by the increasing of irradiation time. When the irradiation time was more

than 150 min for AV 43 and 240 min for PNP, the increase of the photodegradation ratio was not obvious. The optimal photodegradation conditions were: pH 3.0, CQDs/P25 1.0 g/L for AV 43 and 2.0 g/L for PNP, and irradiation time 150 min for AV 43 and 240 min for PNP. Compared with the pure P25, the degradation ratio of AV 43 (0.15 mmol/L) and PNP (30 mg/L) could be enhanced from 60% to 93% and from 89% to 96%, respectively. After five times circles, the photocatalytical performance of CQDs/P25 was same as its first use, because surface modification of TiO_2 by –COOTi- group could be stable for the photodegradation of aromatic pollutants.[3-5] The enhanced photodegradation activity should be attributed to the existence of CQDs, because: (a) CQDs narrowed the band gap of the CQDs/TiO_2 nanocomposites, (b) the electron-hole separation of CQDs/P25 could be excited by lower energy than that of P25, (c) the light absorption range of P25 was expanded into visible light by accelerating the photogenerated electron transfer from CQDs to P25, and (d) the separation process of the photoexcited electron-hole pairs could be improved by CQDs as an electron pool. This visible light degradation mechanism was demonstrated in the UV-Vis diffuse reflection absorption spectra and XPS analysis.

Fig. 9

Acknowledgments

This work was supported by the National Natural Science Foundation of China (20977074 and 21175115), the Program for New Century Excellent Talents in University (NCET-11 0904), Outstanding Youth Science Foundation of Fujian Province, China (2010J06005), and the Science & Technology Committee of Fujian Province, China (2012Y0065).

References

1 J. M. Herrmann, C. Duchamp, M. Karkmaz, B. T. Hoai, H. Lachheb, E. Puzenat, Guillard C, *J. Hazard. Mater*., 2007, **146**, 624-629.

2 S. Jõks, D. Klauson, M. Krichevskaya, S. Preis, F. Qi, A. Weber, A. Moiseev, J. Deubener, *Appl. Catal. B*, 2012, **111-112**, 1-9.

3 S. X. Li, S. J. Cai, F. Y. Zheng, *Dyes Pigments*, 2012, **95**, 188-193.

4 S. X. Li, F. Y. Zheng, W. L. Cai, A. Q. Han, Y. K. Xie, *J. Hazard. Mater.*, 2006, **135,** 431-436.

5 S. X. Li, F. Y. Zheng, X. L. Liu, F. Wu, N. S. Deng, J. H. Yang, *Chemosphere*, 2005, **61**, 589-594.

6 B. R. Hyun, Y. W. Zhong, A. C. Bartnik, L. Sun, H. D. Abruňa, F. W. Wise, J. D. Goodreau, J. R. Mattews, T. M. Leslie, N. F. Borrelli, *ACS Nano*, 2008, **11**, 2206-2212.

7 G. S. Wu, M. Tian, A. C. Chen, *J. Photochem. Photobiol. A*, 2012, **233**, 65–71.

8 N. Guijarro, T. Lana-Villarreal, I. Mora-Seró, J. Bisquert, R. Gómez, *J. Phys. Chem. C*, 2009, **113**, 4208–4214.

9 Q. Wang, X. Yang, L. Chi, M. Cui, *Electrochimica Acta*, 2013, **91**, 330-336.

10 A. M. Derfus, W. C. W. Chan, S. N. Bhatia, *Nano Lett*, 2004, **1,** 11-18.

11 S. N. Baker, G. A. Baker, *Angew. Chem. Int. Ed.*, 2010, **49**,

6726-6744.

12 H. T. Li, X. D. He, Z. H. Kang, Y. Liu, Y. S. Lian, C. H. A. Tsang, X. B. Yang, S. T. Lee, *Angew Chem Int Ed.*, 2010, **49**, 4430–4434.

13 J. G. Zhou, C. Booker, R. Y. Li, X. T. Zhou, T. K. Sham, X. L. Sun, Z. F. Ding, *J. Am. Chem. Soc.*, 2007, **129**, 744-745.

14 S. X. Li, J. Z. Zheng, D. J. Chen, Y. j. Wu, W. X. Zhang, F. Y. Zheng, J. Cao, Y. L. Liu, *Nanoscale*, 2013, **5**, 11718-11724.

15 J. Z. Zheng, S. F. Li, W. X. Zhang, J. Cao, S. X. Li, Z. M. Rao, *Analyst*, 2013, **138**, 916-920.

16 J. Z. Zheng, Z. J. Xue, S. F. Li, S. X. Li, Z. M. Rao, *Analytical Methods*, 2012, **4**, 2791-2796.

Figure captions

Fig. 1 TEM images of carbon quantum dots (CQDs) and CQDs/TiO_2: (a) TEM image of CQSs; (b) HRTEM image of CQDs; (c) TEM image of CQDs/P25; (d) Magnified TEM images of CQDs/P25

Fig. 2 TGA datum of P25 (a),CQDs/TiO_2 (b) sample and the corresponding calculated loss mass percentage.

Fig. 3 XRD patterns of P25 (a) and CQDs/TiO_2 (b) samples

Fig. 4 FT-IR spectrums of P25 (a) and CQDs/P25 samples (b)

Fig. 5 UV–Vis diffuse reflection absorption spectra of P25 (a), CQDs/P25 (b) and CQDs (c) samples.Fig. 6 The XPS data of Ti 2p in P25 and CQDs/P25 samples

Fig. 7 Photodegradation ratio of acid violet 43 and *p*-nitrophenol with CQDs/TiO_2 catalysts under different pH value. Conditions: temperature 25 °C; catalyst dosage 1.0 g/L; initial concentrations of acid violet 43 and *p*-nitrophenol were 0.15 mmol/L and 30 mg/L, respectively; irradiation time for acid violet 43 and *p*-nitrophenol were 2.5 h and 4.0 h, respectively.

Fig. 8 Photodegradation ratio of acid violet 43 (a) and *p*-nitrophenol (b) with different concentration of CQDs/TiO_2. Conditions: temperature 25 °C; pH 3.0; initial concentrations of acid violet 43 and *p*-nitrophenol were 0.15 mmol/L and 30 mg/L, respectively; irradiation time for acid violet 43 and *p*-nitrophenol were 2.5 h and 4.0 h, respectively.

322 **Fig. 9** Photodegradation ratio of acid violet 43 (a) and *p*-nitrophenol (b)
323 with P25 and CQDs/TiO_2 catalysts for different irradiation time.
324 Conditions: temperature 25 °C; pH 3.0; catalyst dosage of 1.0 g/L and 2.0
325 g/L were used for acid violet 43 and *p*-nitrophenol, respectively; initial
326 concentration of acid violet 43 and *p*-nitrophenol were 0.15 mmol/L and
327 30 mg/L, respectively.
328

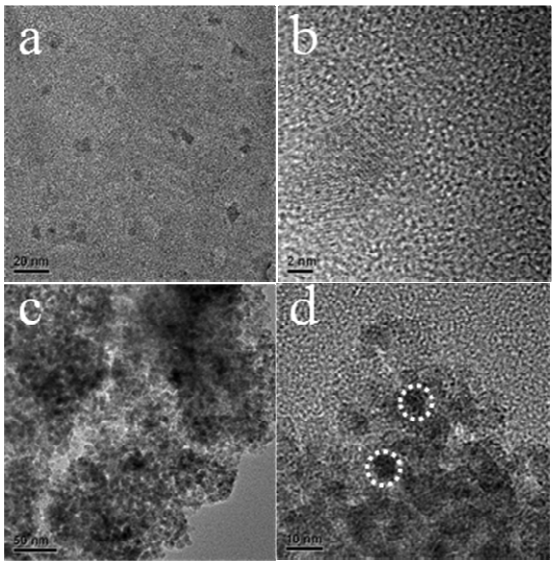

Fig. 1.

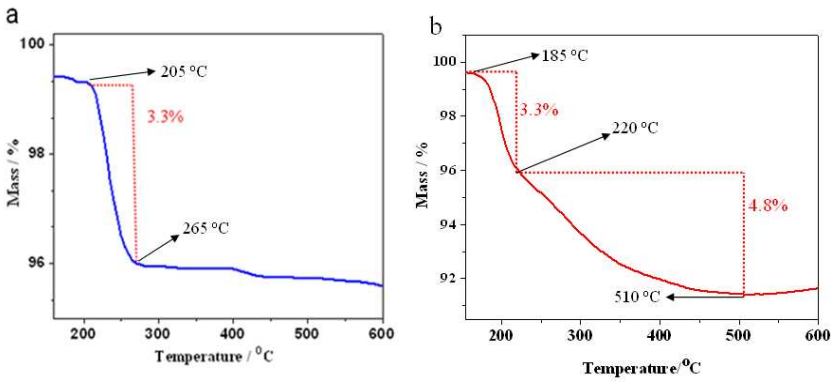

Fig. 2.

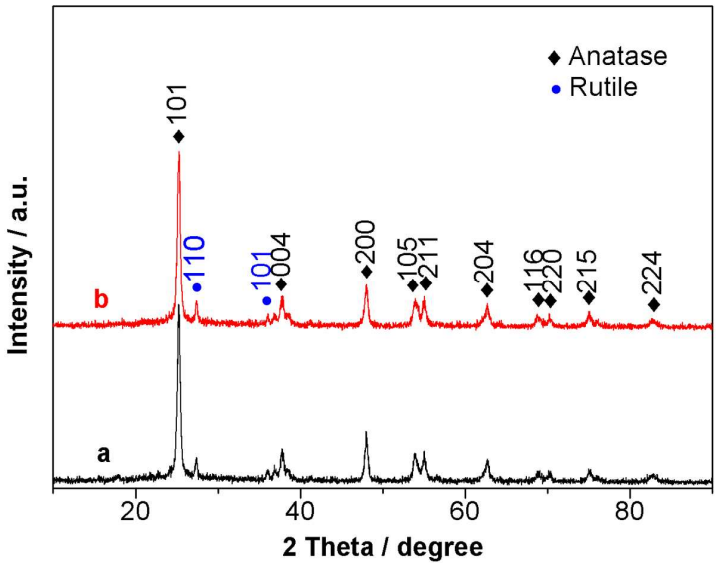

334

335 **Fig. 3.**

336

337

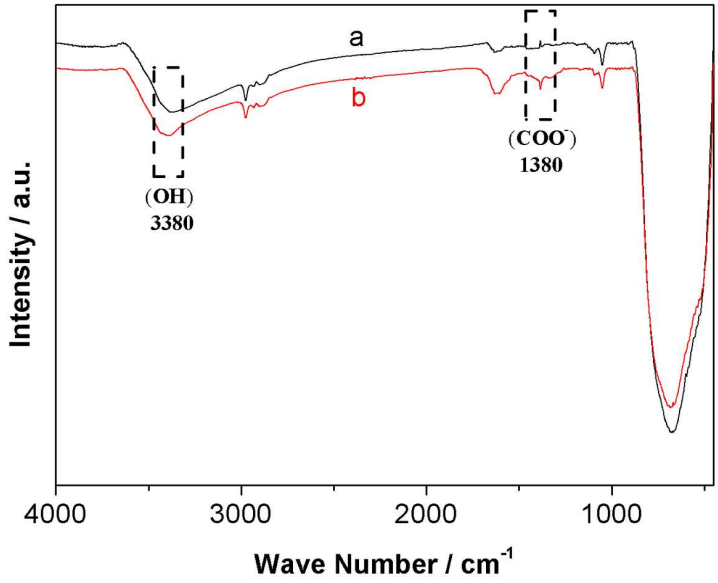

338

339 **Fig. 4.**

340

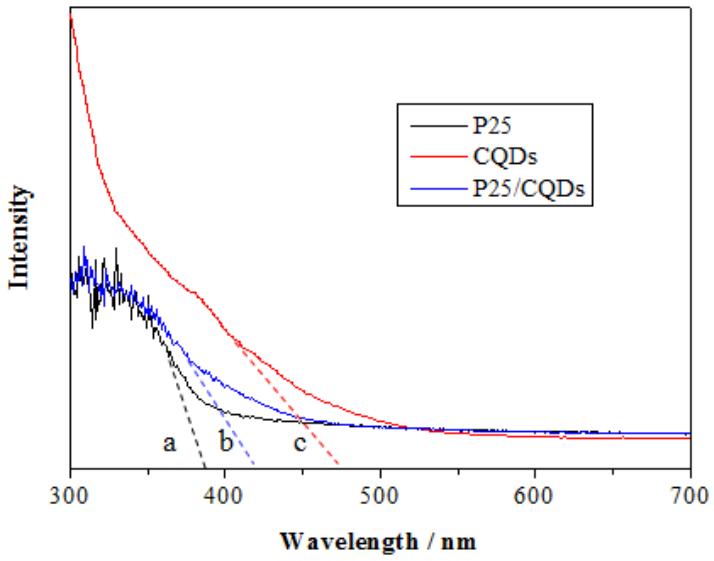

341

342 **Fig. 5.**

343

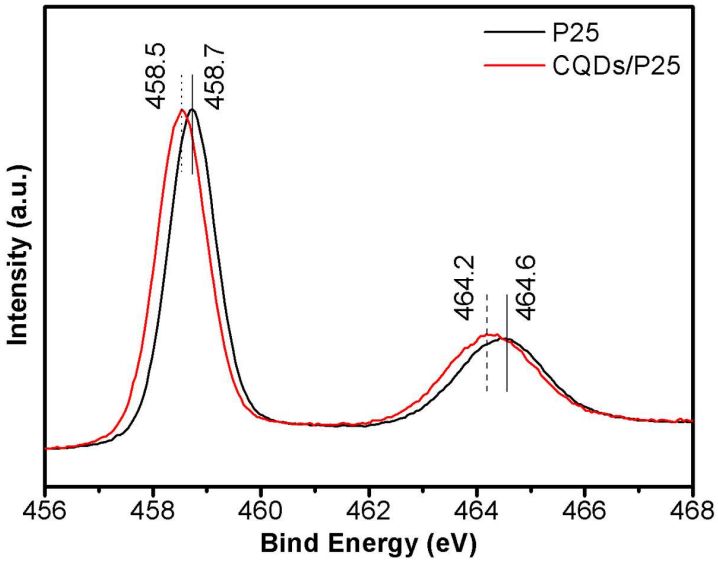

344

345 **Fig. 6.**

346

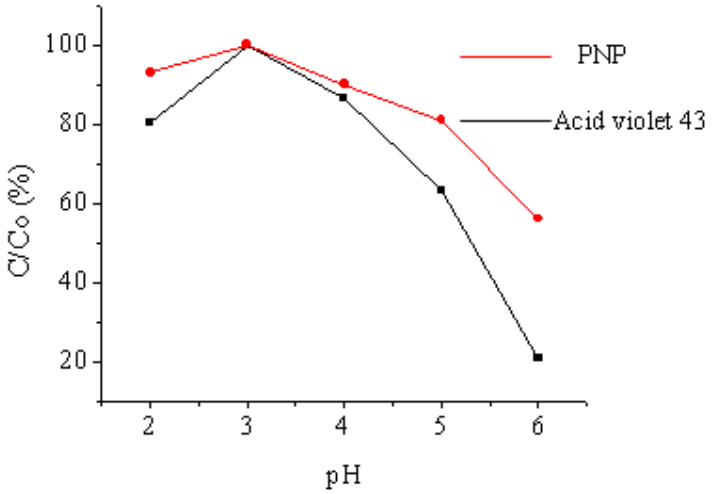

347

348 **Fig. 7.**

349

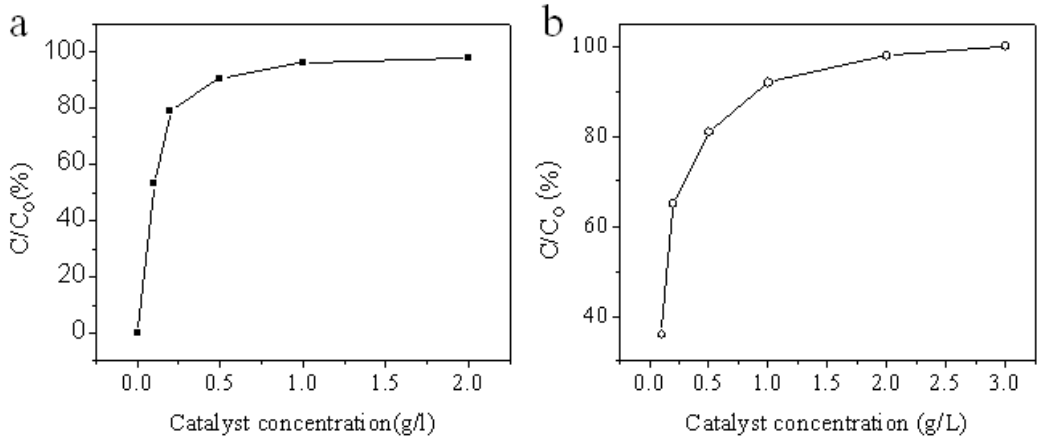

350

351 **Fig. 8.**

352

353

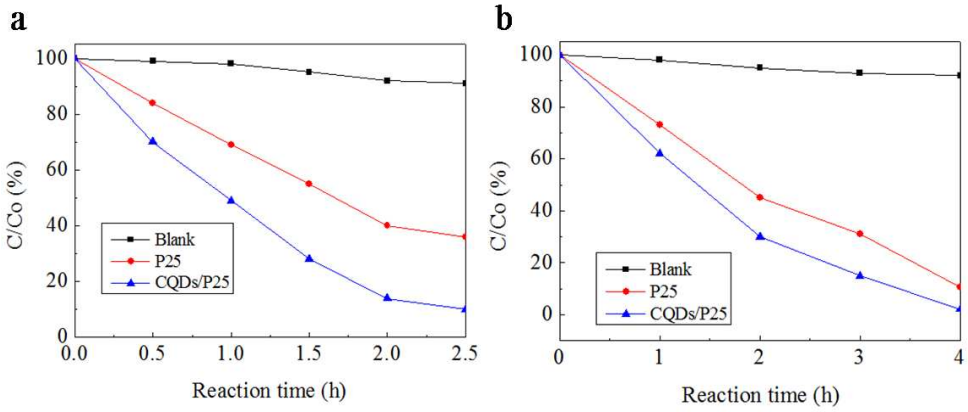

354

355 **Fig. 9.**

356